

Probabilistic Yielding and Cyclic Behavior of Geomaterials

Kallol Sett¹, Boris Jeremić^{2*}

¹ *Department of Civil Engineering, The University of Akron, Akron, OH 44325*

² *Department of Civil and Environmental Engineering, University of California, Davis, CA 95616*

1. ABSTRACT

In this paper, the novel concept of probabilistic yielding is used for 1-D cyclic simulation of the constitutive behavior of geomaterials. Fokker–Planck–Kolmogorov (FPK) equation based probabilistic elastic–plastic constitutive framework is applied for obtaining the complete probabilistic (probability density function) material response. Both perfectly plastic and hardening type material models are considered. It is shown that when uncertainties in material parameters are taken in consideration, even the simple, elastic–perfectly plastic model captures some of the important features of geomaterial behavior, for example, modulus reduction with cyclic strain, which, deterministically, is only possible with more advanced constitutive models. Further, it is also shown that the use of isotropic and kinematic hardening rules does not significantly improve the probabilistic material response.

*Correspondence to: Boris Jeremić, Department of Civil and Environmental Engineering, University of California, One Shields Avenue, Davis, CA 95616, jeremic@ucdavis.edu

KEY WORDS: Soil uncertainty, Elasto–plasticity, Fokker-Planck-Kolmogorov equation, Cyclic behavior

2. INTRODUCTION

Modeling of geomaterials is inherently uncertain. This uncertainty stems from natural variability of geomaterials (spatial uncertainty), and testing and transformation errors (point uncertainty) (Lacasse and Nadim [17], Phoon and Kulhawy [20]). These uncertainties not only affect the failure characteristics of geomaterials, but also the behavior of geostructures, made with geomaterials. Traditionally, geotechnical engineering community deals with uncertainties in geomaterial by applying (large) factor of safety. However, use of large factors of safety results not only in over-expensive design, but also, sometimes, in unsafe structures (cf. Duncan [4]). Hence, in recent years, the geotechnical community has seen an increasing emphasis on probabilistic characterization of soil and subsequent reliability-based design.

One of the important aspects of probabilistic geomechanics simulation that has received less attention is the probabilistic constitutive problem. Among the few published papers were those by Fenton and Griffiths ([7], [8], [9]) on probabilistic simulation of spatially random c - ϕ soil using Monte Carlo technique, and those by Anders and Hori ([1], [2]) on probabilistic simulation of von Mises elastic-perfectly plastic material using perturbation technique. Both Monte Carlo and perturbation techniques have their inherent drawbacks (Matthies et al. [19], Keese [16]) and in dealing with those, recently, Jeremić et al. [13] proposed Eulerian–Lagrangian form of Fokker–Planck–Kolmogorov equation (FPKE) approach (cf. Kavvas [15]) to modeling and simulation for probabilistic elasto–plasticity. FPKE approach to probabilistic elasto–

plasticity not only overcomes the drawbacks associated with other probabilistic simulation techniques, but also is fully compatible with the incremental theory of elasto-plasticity, and hence can easily be applied to probabilistic modeling and simulation of different elastic-plastic constitutive models. Solution strategies for FPK partial differential equation, corresponding to elastic-plastic constitutive rate equation and simulated probabilistic stress-strain responses under monotonic loading, assuming mean stress yielding, were discussed by Sett et al. ([22], [23]) for both linear and non-linear hardening models. The concept of probabilistic yielding was introduced and its effect on constitutive simulation under monotonic loading was discussed by Jeremić and Sett [12]. It was shown that due to uncertainty in yield function (stress), there is always a possibility, depending upon the magnitude of uncertainty, that plastic behavior starts at very very low strain and influence of elastic behavior continues far into plastic domain (at large strains) and hence, the ensemble average (mean) of all the possibilities or the most probable (mode) possibility differ from deterministic behavior. In addition to that, a very realistic, smooth transition between elastic and plastic domains was observed even for elastic perfectly plastic models. Further, nonlinear behavior was observed even for linear hardening models.

In this paper, the concept of probabilistic yielding is extended to 1-D cyclic simulations of geomaterials. Both elastic-perfectly plastic and hardening-type material model are considered. The numerical technique of solving FPKE cyclically with probabilistic yielding is discussed. Simulated responses were discussed in terms of probability density function (PDF) and its statistical moments.

3. FOKKER–PLANCK–KOLMOGOROV APPROACH TO PROBABILISTIC ELASTO–PLASTICITY

The Eulerian–Lagrangian form Fokker–Planck–Kolmogorov equation (cf. Kavvas [15]) corresponding to generalized 1–D constitutive rate equation can be written as (Jeremić et al. [13]):

$$\begin{aligned} \frac{\partial P(\sigma(x_t, t), t)}{\partial t} = & \\ \frac{\partial}{\partial \sigma} \left[\left\{ \left\langle \eta(\sigma, D, \epsilon; x_t, t) \right\rangle + \int_0^t d\tau Cov_0 \left[\frac{\partial \eta(\sigma, D, \epsilon; x_t, t)}{\partial \sigma}; \eta(\sigma, D, \epsilon; x_{t-\tau}, t - \tau) \right] \right\} P(\sigma(x_t, t), t) \right] & \\ + \frac{\partial^2}{\partial \sigma^2} \left[\left\{ \int_0^t d\tau Cov_0 \left[\eta(\sigma, D, \epsilon; x_t, t); \eta(\sigma, D, \epsilon; x_{t-\tau}, t - \tau) \right] \right\} P(\sigma(x_t, t), t) \right] & \end{aligned} \quad (1)$$

where, $P(\sigma(x_t, t), t)$ is the probability density of stress (σ) at (pseudo) time t , and η is the operator variable, obtained by collecting together all the operators and variables on the r.h.s of the generalized constitutive rate equation:

$$\frac{d\sigma(x_t, t)}{dt} = \eta(\sigma, D, \epsilon; x_t, t) \quad (2)$$

In Eq. (2), ϵ is the strain, and D is the tangent modulus, which could be elastic or elastic–plastic:

$$D = \begin{cases} D^{el} & \text{elastic} \\ D^{el} - \frac{D^{el} \frac{\partial U}{\partial \sigma} \frac{\partial f}{\partial \sigma} D^{el}}{\frac{\partial f}{\partial \sigma} D^{el} \frac{\partial U}{\partial \sigma} - \frac{\partial f}{\partial q_*} r_*} & \text{elastic-plastic} \end{cases} \quad (3)$$

where, D^{el} , f , U , q_* , and r_* are elastic modulus, yield surface, plastic potential surface, internal variable(s), and rate(s) of evolution of internal variable(s) respectively.

Eq. (1) is the most general form of elastic–plastic constitutive rate equation, written in probability density space. This equation (Eq. (1)) can be written in a more compact form:

$$\frac{\partial P(\sigma(x_t, t), t)}{\partial t} = \frac{\partial}{\partial \sigma} \{N_{(1)}P(\sigma(x_t, t), t)\} + \frac{\partial^2}{\partial \sigma^2} \{N_{(2)}P(\sigma(x_t, t), t)\} \quad (4)$$

where, $N_{(1)}$ and $N_{(2)}$ are advection and diffusion coefficients respectively, and are material model specific. By specializing Eq. (4) to (any) particular constitutive model, the resulting FPKE can be solved to obtain the probability density function of stress response, given uncertainties in material properties and driving strain. However, difference in material behavior in elastic and elastic-plastic regions necessitates solution of FPKE twice - one corresponding to elastic constitutive equation (with $N_{(1)}^{el}$ and $N_{(2)}^{el}$, the advection and diffusion coefficients corresponding to elastic constitutive equation) and the other corresponding to elastic–plastic constitutive equation (with $N_{(1)}^{ep}$ and $N_{(2)}^{ep}$, the advection and diffusion coefficients corresponding to elastic–plastic constitutive equation). The switch from elastic to elastic–plastic region (solution) can be controlled using mean stress yielding:

$$\begin{aligned} \text{if} \quad & \langle f \rangle < 0 \vee (\langle f \rangle = 0 \wedge d \langle f \rangle < 0) && \text{use elastic FPKE} \\ \text{or, if} \quad & \langle f \rangle = 0 \vee d \langle f \rangle = 0 && \text{use elastic–plastic FPKE} \end{aligned} \quad (5)$$

However, difficulty arises if the material yield parameter(s) are uncertain, as the mean yield criteria then does not account for the complete probabilistic yielding of material. For example, such mean yielding will neglect the possibilities of elastic–plastic behavior in the elastic region and vice versa. The concept of probabilistic yielding overcomes this limitation, as it solves

Eq. (4) once, with equivalent advection and diffusion coefficients, $N_{(1)}^{eq}$ and $N_{(2)}^{eq}$ (Jeremić and Sett [12]):

$$\begin{aligned} N_{(1)}^{eq}(\sigma) &= (1 - P[\Sigma_y \leq \sigma])N_{(1)}^{el} + P[\Sigma_y \leq \sigma]N_{(1)}^{ep} \\ N_{(2)}^{eq}(\sigma) &= (1 - P[\Sigma_y \leq \sigma])N_{(2)}^{el} + P[\Sigma_y \leq \sigma]N_{(2)}^{ep} \end{aligned} \quad (6)$$

where $(1 - P[\Sigma_y \leq \sigma])$ represents the probability of material being elastic, while $P[\Sigma_y \leq \sigma]$ represents the probability of material being elastic–plastic. The probabilities of material being elastic and the probabilities of material being elastic–plastic can easily be calculated from the cumulative density function of yield function (stress).

It is worth noting that the probabilistic yield criterion (Eq. (6)) represents probabilistic restatement of the deterministic yield criteria. The probabilistic yield criteria is introduced (or, the deterministic yield criteria is written in probability space) in order to properly model uncertain (probabilistic) yield strength.

It is also very interesting to note that proposed approach for calculating equivalent advection and diffusion coefficients is similar to the solution strategy of famous Black–Scholes [3] equation in financial engineering modeling of European option, where probabilities of exercise of the (European) option, obtained from cumulative density functions, are multiplied with stock price and present value of option strike price to calculate the option price.

4. ELASTIC–PERFECTLY PLASTIC MATERIAL

In this section, the FPKE–approach, along with the concept of probabilistic yielding, is applied to simulate 1–D (shear stress–shear strain) cyclic behavior of elastic–perfectly plastic material. Only von Mises material model has been considered. It may, however, be noted that presented

development is general enough to be used with any material model and that von Mises is just one such model we use for illustration purposes.

The von Mises yield criteria can be written as:

$$\sqrt{J_2} - k = 0 \quad (7)$$

where, k is a material parameter (yield strength like) and $J_2 = 3/2s_{ij}s_{ij}$ is the second invariant of deviatoric stress tensor $s_{ij} = \sigma_{ij} - 1/3\sigma_{kk}\delta_{ij}$. For 1-D shear, Eq. (7) becomes:

$$|\sigma| - \sigma_y = 0 \quad \text{or} \quad \sigma = \pm\sigma_y \quad (8)$$

The yielding occurs at a yield stress of $\pm\sigma_y$. It, however, is important to note that both σ_y and σ are uncertain and are described by their respective probability density functions. For elastic-perfectly plastic material, the distribution of yield stress (σ_y) is given by its experimentally measured initial distribution, and remains constant. The stress (σ), however, evolves according to the governing FPKE (Eq. (4)) and its distribution is given by the solution of the governing FPKE (Eq. (4)). For 1-D von Mises elastic-perfectly plastic shear constitutive model, the elastic and the elastic-plastic advection and diffusion coefficients of the governing FPKE (Eq. (4)), becomes:

$$\begin{aligned} N_{(1)}^{el} &= \frac{d\epsilon_{xy}}{dt} \langle G \rangle & ; & \quad N_{(2)}^{el} = t \left(\frac{d\epsilon_{xy}}{dt} \right)^2 Var[G] \\ N_{(1)}^{ep} &= 0 & ; & \quad N_{(1)}^{ep} = 0 \end{aligned} \quad (9)$$

where, G is the shear modulus, $d\epsilon_{xy}$ is the (deterministic) incremental shear strain, t is the pseudo time, $\langle \cdot \rangle$ represents expectation operation and $Var[\cdot]$ represents variance operation. The equivalent advection and diffusion coefficients (refer Eq. (6)) for von Mises elastic-perfectly plastic material, then, becomes:

$$\begin{aligned}
N_{(1)}^{eq}(\sigma) &= (1 - P[\Sigma_y \leq \sigma]) \frac{d\epsilon_{xy}}{dt} \langle G \rangle \\
N_{(2)}^{eq}(\sigma) &= (1 - P[\Sigma_y \leq \sigma]) t \left(\frac{d\epsilon_{xy}}{dt} \right)^2 Var[G]
\end{aligned} \tag{10}$$

One may note that, in deriving the elastic and elastic–plastic advection and diffusion coefficients (Eq. (9)), it was assumed that spatial random field material properties (G , and σ_y) would be first discretized into random variables, for example at Gauss points, by appropriate tools, for example Karhunen–Loève expansion (Karhunen [14], Loève [18], Ghanem and Spanos [10]). In other words, the solution of FPKE, with advection and diffusion coefficients given by Eq. (10), represents point–location scale von Mises elastic–perfectly plastic material behavior, and not the local–average material behavior. The local–average material behavior, if sought for, can then be assembled using polynomial chaos expansion (Wiener [27], Ghanem and Spanos [10]).

Probability Density Function: The FPKE (Eq. (4)), with advection and diffusion coefficients given by Eq. (10), was solved incrementally with pseudo time steps using method of lines. The stress domain of the Fokker–Planck–Kolmogorov PDE was discretized first on a uniform grid by central differences, and thereby obtaining a series of ODE. The series of ODEs was then solved, after incorporating boundary conditions, simultaneously and incrementally, with n pseudo time steps, using a standard open–source ODE solver, SUNDIALS [11], which utilizes ADAMS method and functional iteration.

The yield shear strength (σ_y) of the material was assumed to have a mean value of 60 kPa with a COV of 30%, values typical for clay (Federal Highway Administration [6], Lacasse and Nadim [17]). Also, the yield shear strength was assumed to be either normal or Weibull (with shape parameter of 3.31 and scale parameter of 0.067) distribution as shown in Fig. 1.

The shear modulus (G) was also assumed to be either normal or Weibull distribution, but

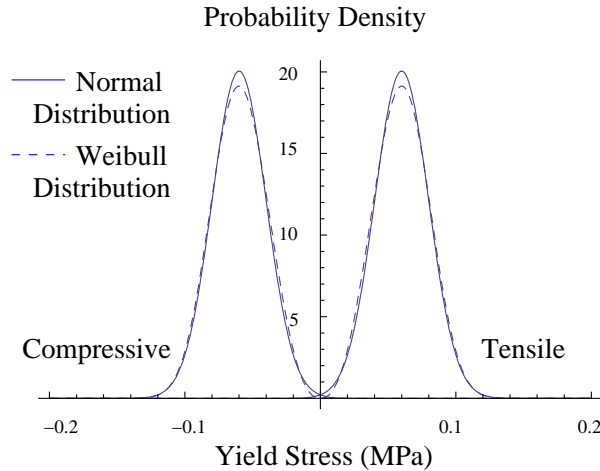


Figure 1. Elastic–perfectly plastic probabilistic model: PDF of yield stress

with a mean value of 100 MPa and a COV of 25%. The cyclic probabilistic von Mises, elastic–perfectly plastic shear stress–shear strain response (evolutionary probability density function (PDF) of shear stress), for the case where both yield shear strength (σ_y) and shear modulus (G) are normally distributed, is shown in Fig. 2. Two different views of the loading–unloading–reloading cycle are shown, focusing on the transition between loading and unloading, and unloading and reloading branches. As can be seen from Fig. 2, PDF for initial stress (a deterministic Dirac delta function at stress–strain origin) advected and diffused into the domain, governed by the advection and diffusion coefficients (Eq. (10)). It is very important to also note that, even–though the deterministic response for von Mises elastic–perfectly plastic material is bi–linear, due to introduced uncertainties in yielding, the probabilistic response is non–linear from the beginning. That is, due to uncertainty in yield strength, there is a (small) possibility that the material becomes elasto–plastic from the very beginning of loading. This

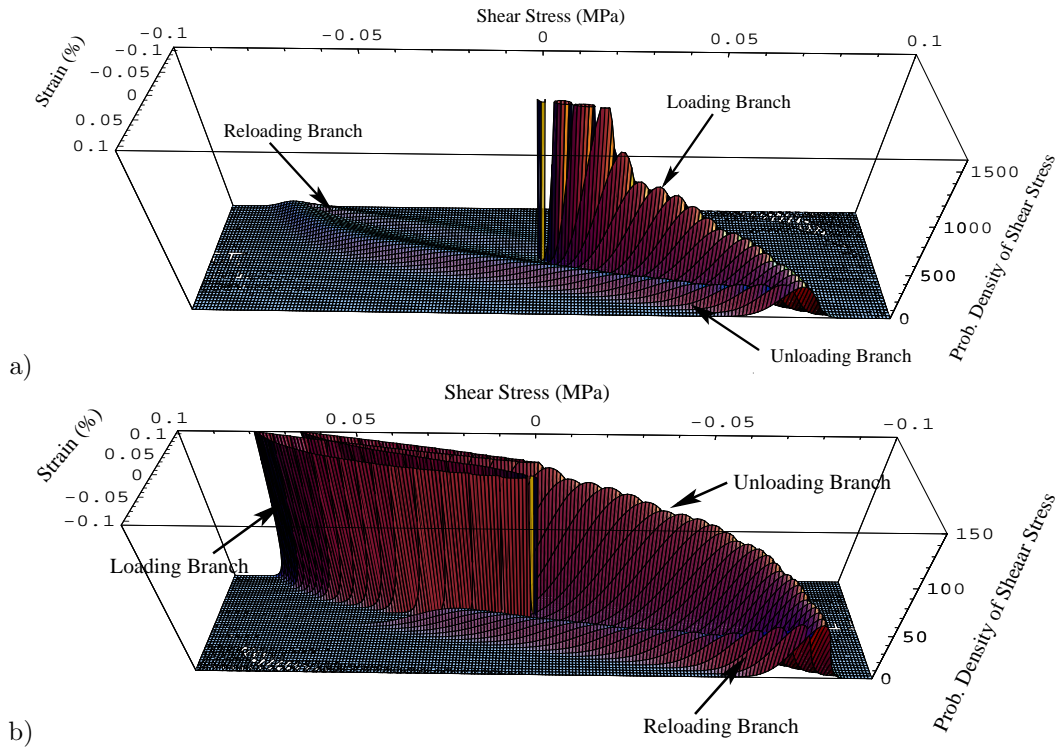


Figure 2. Elastic–perfectly plastic probabilistic model under cyclic loading: evolutionary PDF of shear stress (a) view from the junction of loading and unloading branches (probability densities of shear stress are truncated at a value 1500 for clarity of the plot) and (b) view from the junction of unloading and reloading branches (probability densities of shear stress are truncated at a value of 150 for clarity of the plot)

possibility has been quantified from the PDF of the yield strength and taken into consideration implicitly during simulation using the equivalent advection and diffusion coefficients ($N_{(1)}^{eq}$ and $N_{(2)}^{eq}$, refer Eq. (10)). Those coefficients assigns probability weights to the realizations of stress response based on the probability of material being elastic or elastic–plastic. Initially, in the loading branch, at small strains, the probability of material being elastic–plastic is very small and hence, the initial probabilistic stress response (ensemble of all realizations) is closer (but

not fully) to linear, elastic response. However, as strain increases, the probability of elastic–plastic material behaving increases and the probabilistic stress response gradually becomes more elastic–plastic (Fig. 2(a)).

Upon unloading, the material behaves as (mostly) elastic since elastic–plastic probability weights from the governing PDF of mirror image (negative) of shear strength (Fig. 1) are initially very small. During later stages of unloading (loading in the opposite direction), and similar to the loading branch, the elastic–plastic probability weights increase and gradually transition the response toward elasto–plasticity (Fig. 2(b)). Similar to this, in the subsequent reloading branch, the probability weights are again governed the PDF of (positive, loading branch of) shear strength (Fig. 1), and hence the probabilistic response is again initially more linear, elastic, while gradually it transitions to full elasto–plasticity.

Case of Increasing Strain Loops: In Fig. 3, the evolutionary PDF of shear stress for von Mises elastic–perfectly plastic material (refer Fig. 2) is plotted in terms of its statistical moments – the evolutionary mean (Fig. 3(a)), and standard deviation (Fig. 3(b)) of shear stress – for the first couple of cycles with increasing strain loops. The mean response, when both the yield shear strength (σ_y) and the shear modulus (G) are modeled as Weibull distribution, is also shown in Fig. 3(a). The oscillations in the evolution of standard deviation of shear stress with shear strain are due to step size issue, inherent to the forward Euler method that has been used in solving the FPKE. Work is underway to implement linearly implicit mid-point rule for solving the FPKE corresponding to elastic-plastic constitutive rate equation.

The very important observation that can be made using Fig. 3(a) is that, if one consider uncertainties in geomaterial properties, even the simplest elastic–perfectly model, captures some of the very important features of geomaterial behaviors. For example, reduction of

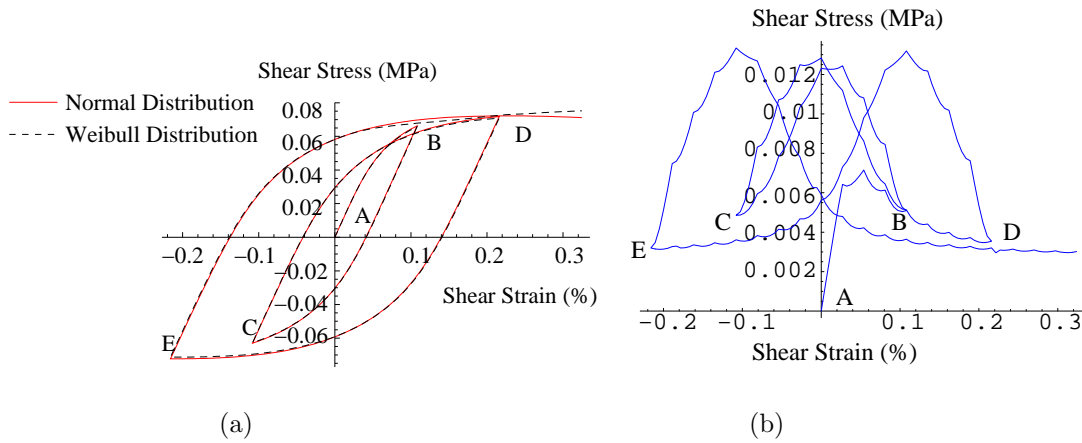


Figure 3. Elastic–perfectly plastic probabilistic model under cyclic loading with increasing strain loops: evolution of (a) mean and (b) standard deviation of shear stress

(secant) modulus with cyclic strain, commonly observed in soil (cf. Vucetic and Dobry [26]), is fairly nicely captured. If using deterministic models, this feature can only be somewhat successfully modeled with fairly complex models, which require many more parameters. It is important to remark that for our probabilistic modeling, (only) statistical distributions (probability density functions) of shear modulus (G) and shear strength (σ_y), are needed. Expansion of elastic–plastic modeling into probability space seems to have added significant new capabilities to modeling.

Case of Constant Strain Loops: This von Mises elastic–plastic material, however, didn’t exhibit (secant) modulus degradation, commonly observed in clay (cf. Vucetic and Dobry [25]), when the material is cycled repeatedly at the same strain. Fig. 4(a) shows such probabilistic response (mean of shear stress). The material was cycled repeatedly up to 0.2% strain. Only first three cycles are shown. It is important to note that the von Mises mean elastic–plastic material behavior is function of both the mean and standard deviation of both shear modulus

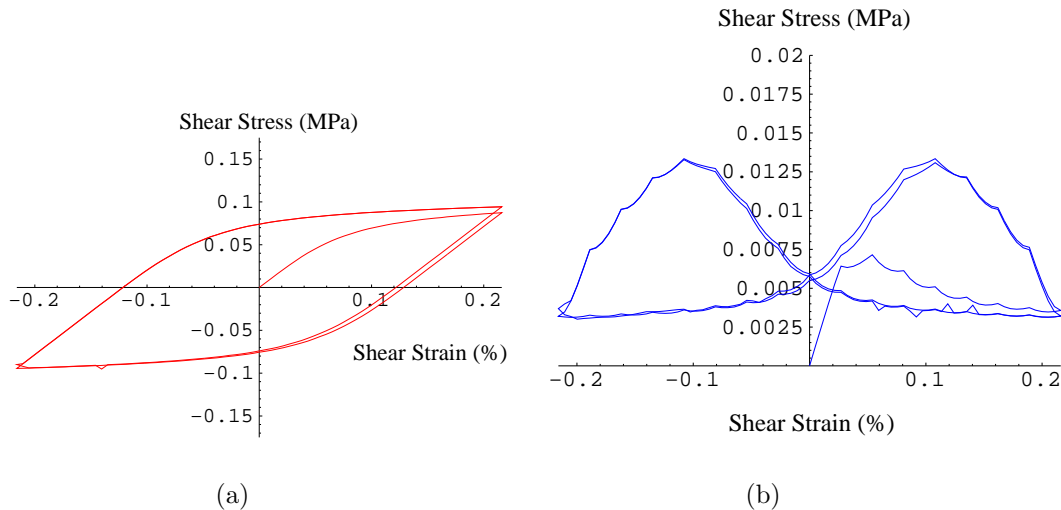


Figure 4. Elastic-perfectly plastic probabilistic model under cyclic loading with all equal loops: evolution of (a) mean and (b) standard deviation of shear stress

(G) and yield shear strength (σ_y). The same von Mises elastic-perfectly plastic model with a different set of material properties could, however, be able to capture the degradation of mean (secant) shear modulus. For example, Japanese stiff clay, when modeled as von Mises elastic-perfectly plastic material, exhibited modulus degradation with number of cycles (Sett et al. [24])

Monotonic Loading: For completeness of comparison, the monotonic behavior of this probabilistic von Mises perfectly plastic material is also shown (refer Fig. 5). As can be observed from Fig. 5(a), the mean shear stress non-linearly increases with shear strain before reaching the perfectly plastic state.

Physically, one may visualize the probabilistic soil constitutive response as an ensemble of the behaviors of infinite number of soil particles in a representative volume element (RVE), for example, a laboratory soil specimen. The behavior of an individual soil particle in a RVE is

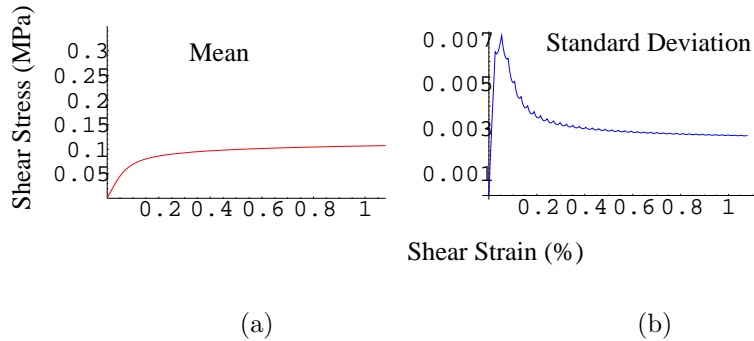


Figure 5. Elastic–perfectly plastic probabilistic model under monotonic loading: evolution of (a) mean, (b) standard deviation, and (c) mean \pm standard deviation of shear stress

governed, in case of elastic–perfectly plastic material, by its modulus and strength. However, if the modulus and strength of each particle are different, for example, governed by their respective PDF, then each particle would behave differently. The PDF of the response behavior then represents the ensemble of all such behaviors, with their respective probability weights. The mean, on the other hand, represents the ensemble average of all such behaviors. In this context, it is important to note that the behaviors presented in this paper do not take into account the correlation between soil particles (scale effect). The scale effect can be accounted for, among others, using stochastic elastic–plastic finite element technique. Sett [21] proposed one such finite element method by extending the spectral approach to stochastic finite element (cf. Ghanem and Spanos [10]) to elastic–plastic problems by updating the material properties at Gauss integration points using the FPKE approach, as the material plastifies.

Further to the promise of an alternate approach to geomaterial modeling, probabilistic approach also quantifies our confidence in the simulated behavior of geomaterials. FPKE based probabilistic elasto–plasticity solves for second-order accurate evolutionary PDF of shear stress (Fig. 2). Ability to obtain the PDF of stress accurately is very important in failure simulation

of geomaterials, as they often fail at low probabilities (tails of PDF). A full PDF contains enormous amount of information. From the PDF, other than the statistical moments, other useful engineering information, for example, the probability of exceedance, most probable solution, as well as some derivative application like sensitivity analysis can be easily obtained or derived. Figs. 3(b) and 4(b) show one of the important confidence measuring parameters, the evolutionary standard deviation of shear stress (square-root of second moment of the evolutionary PDF of shear stress (Fig. 2)), for cyclic responses with increasing loops and all equal loops, respectively. As can be observed from the above figures (Figs. 3(b) and 4(b)), inside any branch (loading, unloading, re-loading, re-unloading, ...), as well as in Fig. 5(b), where the monotonic response is shown, the standard deviation, first increases and then decreases. This is because, initially, when the material is mostly elastic, both the uncertainties in shear modulus (G) and yield strength (σ_y) are governing. As material becomes mostly elastic-plastic, the influence of uncertainty in shear modulus (G) decreases. However, it is important to note that this type of standard deviation response is not generic to all von Mises elastic-perfectly plastic material. The standard deviation response is very much dependent on the amount uncertainties present in both shear modulus (G) and yield strength (σ_y). For example, Fig. 6(b), shows probabilistic response of cyclic behavior of the same material model, except that COV of yield strength (σ_y), is now assumed to be 300%. The standard deviation response shown here is always increasing which is completely different from what was observed in previous case (Figs. 3(b), 4(b) and 5(b)). This is because, for this material, the COV of shear modulus (assumed 30%) is non-significant, compared to the COV of yield strength (assumed 300%), and hence, the standard deviation response (Fig. 6(b)) is predominantly influenced by the uncertainty in yield strength (σ_y). Similar standard deviation response can be observed in

Fig. 7(b), where the material with large COV of yield strength was subjected to monotonic loading.

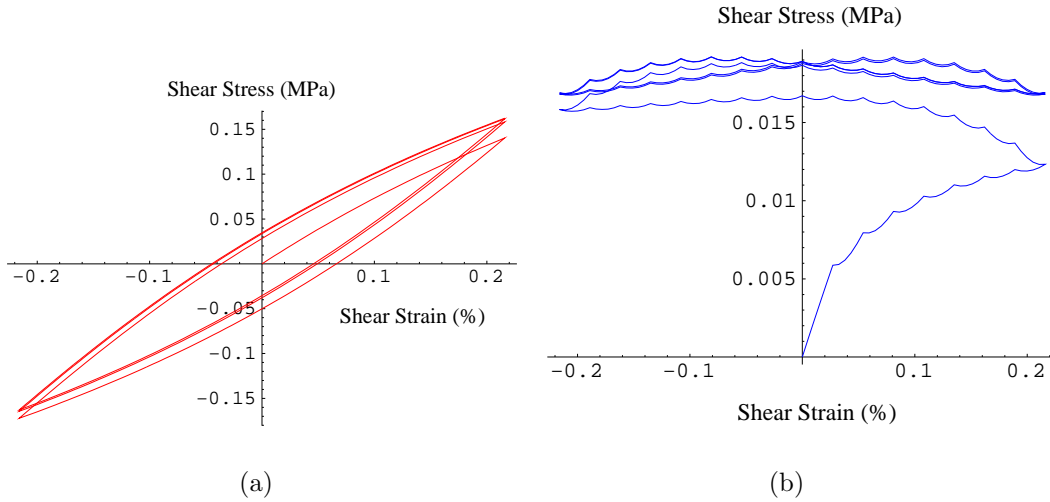


Figure 6. Elastic–perfectly plastic probabilistic model under cyclic loading with all equal loops (probabilistic model parameters are exactly the same as used for simulation in Fig. 4, but with very large yield uncertainty): evolution of (a) mean and (b) standard deviation of shear stress

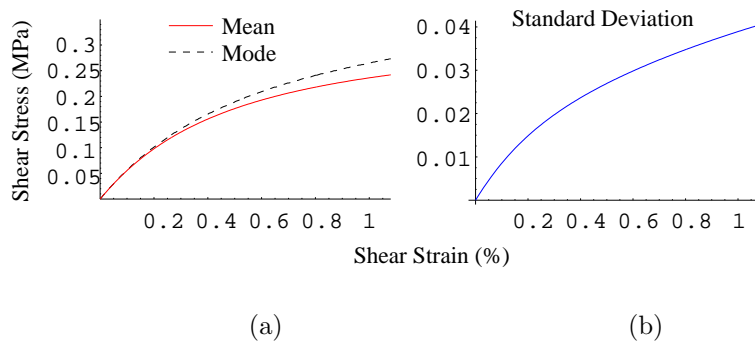


Figure 7. Elastic–perfectly plastic probabilistic model under monotonic loading (model parameters are exactly the same as used for simulation in Fig. 5, but with very large yield uncertainty): evolution of (a) mean, mode, (b) standard deviation, and (c) mean \pm standard deviation of shear stress

It is also interesting to compare Figs. 4(a) and 6(a). Both are mean responses of von Mises

elastic–perfectly plastic material model with same material parameters, except with different COV of yield strength. COV of yield strength for simulation in Fig. 4(a) was 30% and that for simulation in Fig. 6(a) was 300%. It is observed that a completely different responses were obtained. The effect of COV of yield strength on monotonic mean behavior can, similarly, be compared in Figs. 5(a) and 7(a).

5. HARDENING MATERIAL

In this section, the influence of probabilistic yielding is evaluated on cyclic responses of isotropic and kinematic hardening materials. To this end, the same example, as discussed in the previous section (Section 4) is used but with appropriate hardening rule – isotropic or kinematic.

The main difference between the simulations shown in Section 4 for elastic–perfectly plastic material is that for a hardening material the internal variables (q_* , refer Eq. (3)) will evolve as the material plastifies. Such evolution (change) of internal variables is here assumed to be a function of plastic strain. The FPKE that govern the probabilistic evolution of internal variable (q) can be written, in most the general form, as:

$$\frac{\partial P(q(x_t, t), t)}{\partial t} = \frac{\partial}{\partial q} \left\{ N_{(1)IV}^{eq} P(q(x_t, t), t) \right\} + \frac{\partial^2}{\partial q^2} \left\{ N_{(2)IV}^{eq} P(q(x_t, t), t) \right\} \quad (11)$$

where, $N_{(1)IV}^{eq}$ and $N_{(2)IV}^{eq}$ are the equivalent advection and diffusion coefficients, respectively, for the internal variable. As explained for the case of probabilistic stress response for elastic–perfectly plastic material (refer Section 4), since point–location scale FPKE will be solved, the equivalent advection and diffusion coefficients for the internal variable, $N_{(1)IV}^{eq}$ and $N_{(2)IV}^{eq}$, can

be written as:

$$\begin{aligned}
 N_{(1)IV}^{eq}(q) &= P[\Sigma_y \leq \sigma(q)] \frac{d\epsilon_{xy}}{dt} \left\langle \frac{Gr}{G + \frac{1}{\sqrt{3}}r} \right\rangle \\
 N_{(2)IV}^{eq}(q) &= P[\Sigma_y \leq \sigma(q)] t \left(\frac{d\epsilon_{xy}}{dt} \right)^2 \text{Var} \left[\frac{Gr}{G + \frac{1}{\sqrt{3}}r} \right]
 \end{aligned} \tag{12}$$

where, r is the rate of evolution of internal variable (q) with plastic strain. One may note that in the above equivalent advection and diffusion coefficients (Eq. (12)), the contributions of probability weights that the material being elastic are absent. This is because the evolution rule of internal variable is governed by the plastic component of strain only. The equivalent advection and diffusion coefficients for shear stress ($N_{(1)}^{eq}$ and $N_{(2)}^{eq}$) for hardening-type materials, will have contributions from both elastic and plastic components, just like the elastic-perfectly plastic case. However, unlike the elastic-perfectly plastic case, those ($N_{(1)}^{eq}$ and $N_{(2)}^{eq}$) will contain the hardening terms:

$$\begin{aligned}
 N_{(1)}^{eq}(\sigma) &= \frac{d\epsilon_{xy}}{dt} \left[(1 - P[\Sigma_y \leq \sigma]) \langle G \rangle + P[\Sigma_y \leq \sigma] \left\langle G - \frac{G^2}{G + \frac{1}{\sqrt{3}}r} \right\rangle \right] \\
 N_{(2)}^{eq}(\sigma) &= t \left(\frac{d\epsilon_{xy}}{dt} \right)^2 \left[(1 - P[\Sigma_y \leq \sigma]) \text{Var}[G] + P[\Sigma_y \leq \sigma] \text{Var} \left[G - \frac{G^2}{G + \frac{1}{\sqrt{3}}r} \right] \right]
 \end{aligned} \tag{13}$$

To obtain the probabilistic response of von Mises hardening material, the FPKE for probabilistic evolution of internal variable (Eq. (11), with advection and diffusion coefficients given by Eq. (12)) needs to be solved incrementally. This solution needs to be done simultaneously with the FPKE for probabilistic evolution of shear stress (Eq. (4), with advection and diffusion coefficients given by Eq. (13)). Those, in turn, need also to be solved incrementally, with the yield strength random variable (Σ_y) in Eqs. (12) and (13) being updated after each incremental step.

5.1. Isotropic Hardening

For von Mises isotropic hardening material, the yield strength (σ_y) is the internal variable. Yield strength will evolve probabilistically with plastic strain, following Eq. (11), with advection and diffusion coefficients given by Eq. (12). The shear stress, on the other hand, evolves in accordance with Eq. (4), with advection and diffusion coefficients given by Eq. (13).

Fig. 8 shows the evolutionary mean and standard deviation of shear stress during first couple of loading–unloading cycles for von Mises isotropic hardening material with a non-dimensional rate of evolution of internal variable (yield strength, in this case) of 10. All other material parameters are assumed to be the same as used for simulation of elastic–perfectly plastic material in the previous section (Section 4).

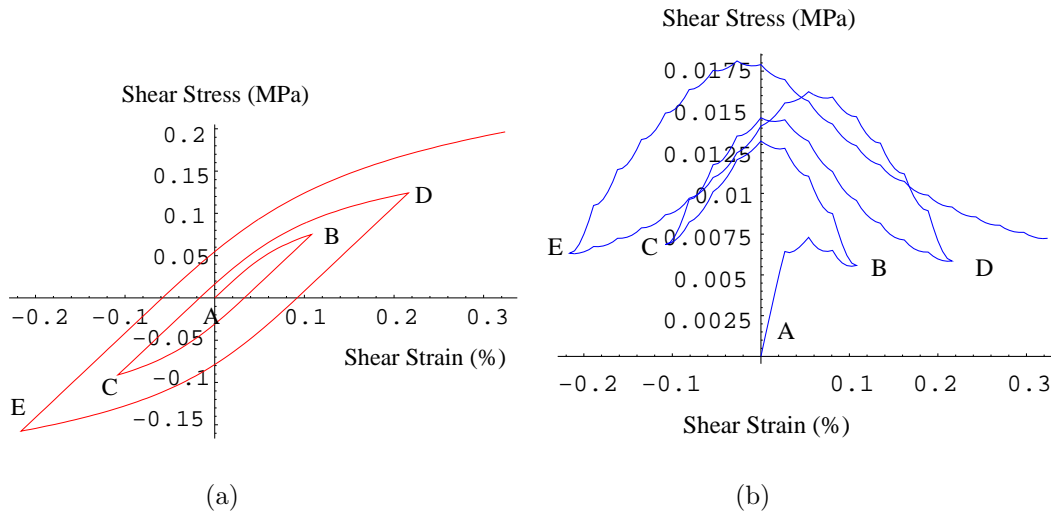


Figure 8. Isotropic hardening probabilistic model under cyclic loading with increasing loops: evolution of (a) mean and (b) standard deviation of shear stress

The evolved PDFs of yield strength after each branch (loading, unloading, re-loading, and re-unloading) are shown in Fig. 9. The initial PDFs of yield strength (positive for loading

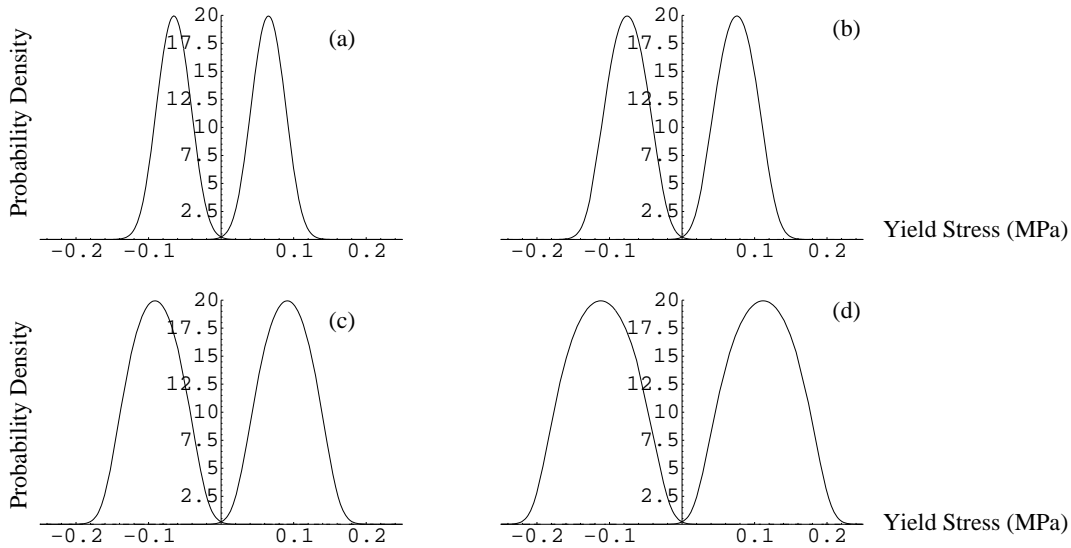


Figure 9. Isotropic hardening probabilistic model under cyclic loading with increasing loops: evolved PDF of yield stress after (a) loading branch, (b) unloading branch, (c) re-loading branch, and (d) re-unloading branch

branch and negative for unloading branch) are the same as assumed for elastic–perfectly plastic material in Section 4 (refer Fig. 1). As expected (and prescribed by the isotropic hardening model), the yield strength evolved (grew) isotropically. However, it is interesting to note the change in probability distributions of yield strength. The normally distributed initial PDFs of yield strength (Fig. 1) evolved into much dispersed non-Gaussian distributions having low kurtosis. In other words, when the material is cycled through loading–unloading cycles, the uncertainty in yield strength increases. Mathematically, increase in uncertainty of shear strength is due to the nonlinearity in formulation of probabilistic yielding, that is, the state variable q appears in both advection and diffusion equations (refer Eq. (12)), and in the evolution equation for internal variable (Eq. (11)).

When comparison is made between Figs. 8 and 3, one can clearly see that, in simulating

cyclic behaviors of geomaterials, isotropic hardening model (Fig. 8) performed, as expected, poorly. That is, the elastic–perfectly plastic probabilistic model (Fig. 3) captures (PDF of) stress–strain loops in a much more realistic way. However, for completeness of comparison, the behavior of isotropic hardening material, when it was cycled to same level (Fig. 10) and when loaded monotonically (Fig. 11) are also shown.

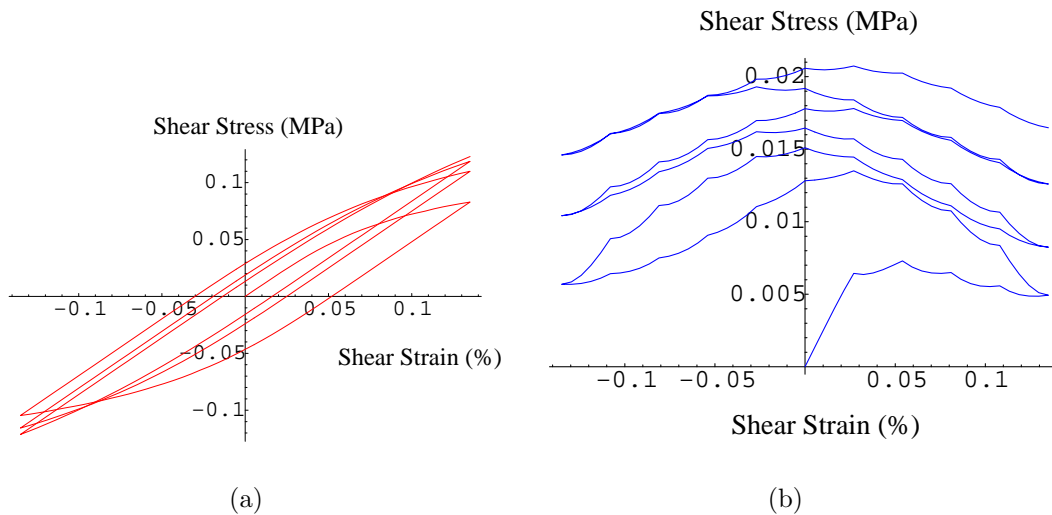


Figure 10. Isotropic hardening probabilistic model under cyclic loading with equal loops: evolution of (a) mean and (b) standard deviation of shear stress

It is noted that monotonic loading curves for both perfectly plastic probabilistic model (Fig. 5) and linear isotropic hardening probabilistic model (Fig. 11) do look similar (with a noted difference of more pronounced hardening for a hardening model), but the real difference in stress–strain predictions with both probabilistic models becomes obvious in the case of cyclic loading.

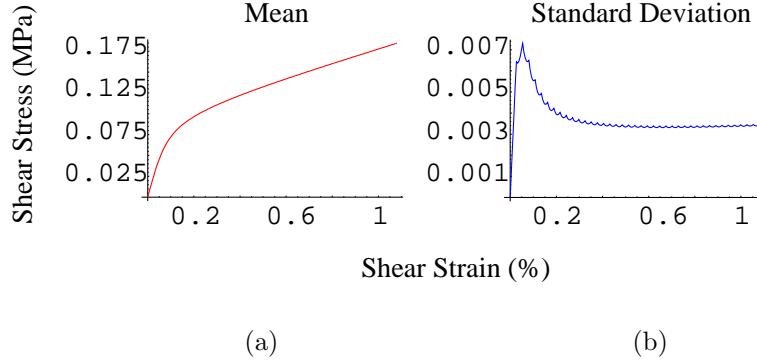


Figure 11. Isotropic hardening probabilistic model under monotonic loading: evolution of (a) mean, (b) standard deviation, and (c) mean \pm standard deviation of shear stress

5.2. Kinematic Hardening

Expanding on elastic–plastic hardening probabilistic models, we now focus on a simple linear kinematic hardening rule based on evolution of back stress (α). By introducing back stress (α) to von Mises yield criteria, one can write:

$$\sqrt{J_\alpha} - k = 0 \quad (14)$$

where, k is again material parameter (yield strength like) and $J_\alpha = 3/2(s_{ij} - \alpha_{ij})(s_{ij} - \alpha_{ij})$ is the α -modified second invariant of deviatoric stress tensor (s_{ij}). For 1-D shear, Eq. (14) becomes:

$$|\sigma - \alpha| - \sigma_y = 0 \quad \text{or} \quad \sigma = \alpha \pm \sigma_y \quad (15)$$

Hence, for kinematic hardening material, the yielding occurs at a stress of $\alpha \pm \sigma_y$, termed in the following as the equivalent yield stress. Initially, α is zero, and σ_y is assumed to have a mean value of 60 kPa with a standard deviation of 20 kPa, resulting in equivalent yield

stress of 60 kPa with a COV of 30%, same as the assumed yield stress for the elastic–perfectly plastic material in Section 4 and isotropic hardening material in Section 5.1. However, the same distribution of equivalent yield stress will be obtained, if one transfers the initial uncertainty from σ_y to α . In other words, a deterministic σ_y of 60 kPa, and an uncertain α of zero mean and a standard deviation of 20 kPa will result in the same equivalent yield stress. The advantage of keeping σ_y deterministic is that it will simplify the probabilistic addition/subtraction in Eq. (15), while estimating the equivalent yield stress after each incremental step of the governing FPKEs, once the back stress (α), the internal variable for kinematic hardening material, starts evolving.

In this study, the back stress (α) is assumed to evolve with plastic strain and hence, it would evolve probabilistically similar to probabilistic evolution of the yield strength for isotropic hardening material. Probabilistic evolution of the back stress will occur according to Eq. (11), with advection and diffusion coefficients given by Eq. (12). Shear stress evolves according to Eq. (4), with advection and diffusion coefficients given by Eq. (13). One may note that the yield strength random variable (Σ_y), appearing in Eqs. (12) and (13), is the equivalent yield strength and is given by Eq. (15). Fig. 12 shows the probabilistic evolution of shear stress in terms of mean, mode, and standard deviation, when a kinematic hardening material[†], was cycled couple of times with increasing strain loops. All other material parameters are assumed to be the same as for the elastic–perfectly plastic material in Section 4. The evolved PDFs of the back stress (α) at the beginning and end of each branch (loading, unloading, re–loading, and re–unloading) are shown in Fig. 13. The evolved PDFs of equivalent yield stress (refer Eq. (15))

[†]with non–dimensional rate of evolution of back stress with plastic strain of 10.

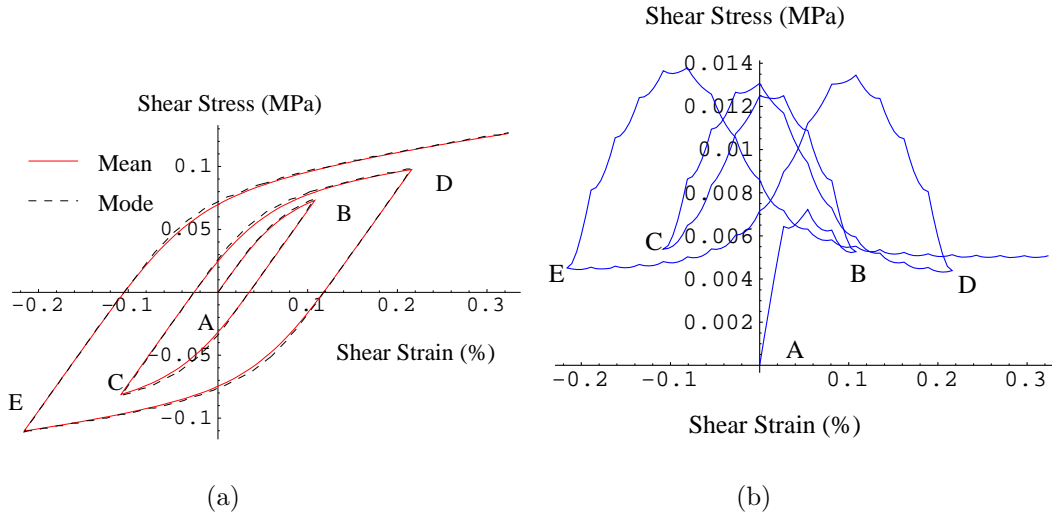


Figure 12. Kinematic hardening probabilistic model under cyclic loading with increasing loops: evolution of (a) mean, mode and (b) standard deviation of shear stress

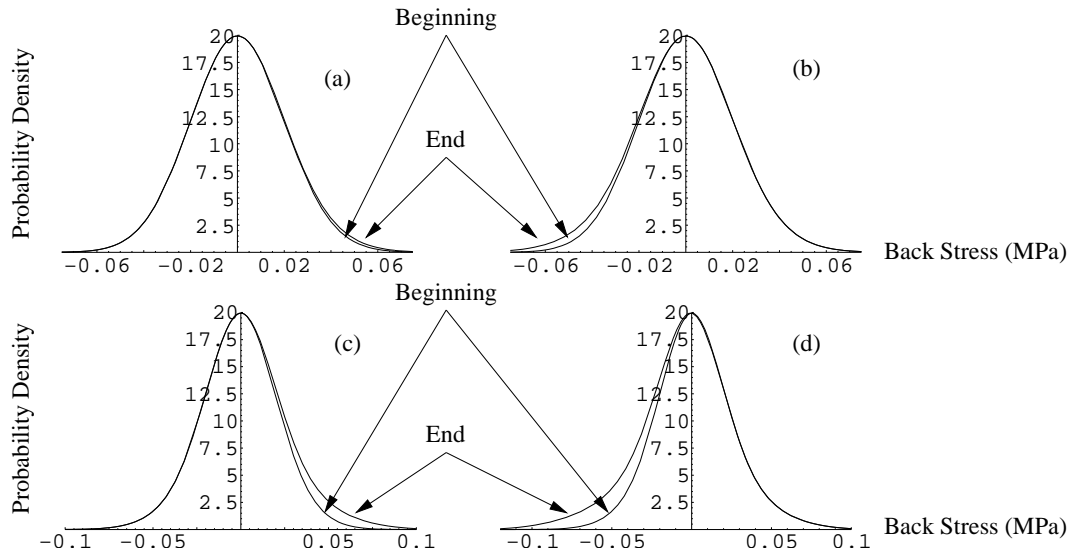


Figure 13. Kinematic hardening probabilistic model under cyclic loading with increasing loops: evolved PDF of back stress at the beginning and end of (a) loading branch, (b) unloading Branch, (c) re-loading branch, and (d) re-unloading branch

after each loading branch are shown in Fig. 14. Similar to the isotropic hardening case the

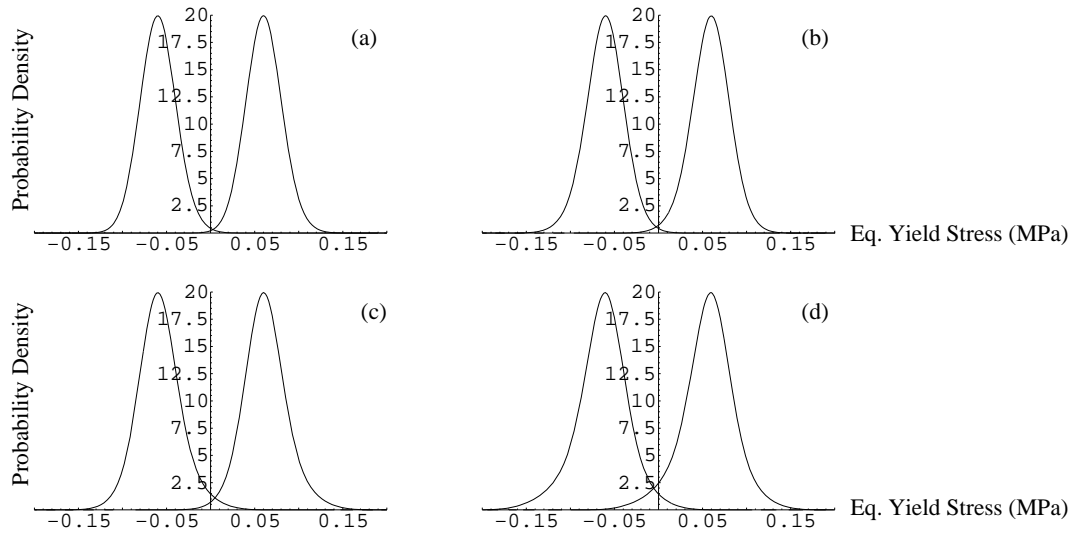


Figure 14. Kinematic hardening probabilistic model under cyclic loading with increasing loops: evolved PDF of equivalent yield stress after (a) loading branch, (b) unloading branch, (c) re-loading branch, and (d) re-unloading branch

uncertainty in (equivalent) yield strength increased as the material was cycled through, but unlike the isotropic hardening model, kinematic hardening model resulted in high kurtosis PDFs of (equivalent) yield strength. It is noted that the cyclic shear stress response of kinematic hardening material (Fig. 12), was more realistic than isotropic hardening material (Fig. 8), however, it didn't differ much from elastic-perfectly plastic material response (Fig. 3). Qualitatively, those, the elastic-perfectly plastic and the kinematic hardening responses, are similar. Like the elastic-perfectly plastic material, for kinematic hardening material, the mean and mode of the evolutionary shear stress (refer Fig. 12) are different, although not significantly.

Similarly, when one compares response (mean and standard deviation of shear stress) for loading cycles to the same strain level, for (i) elastic-perfectly plastic, (Fig. 4), (ii) isotropic

linear hardening (Fig. 10), and (iii) linear kinematic hardening (Fig. 15), probabilistic material models, one can easily observe the qualitative similarity between elastic–perfectly plastic (i) and kinematic hardening responses (iii).

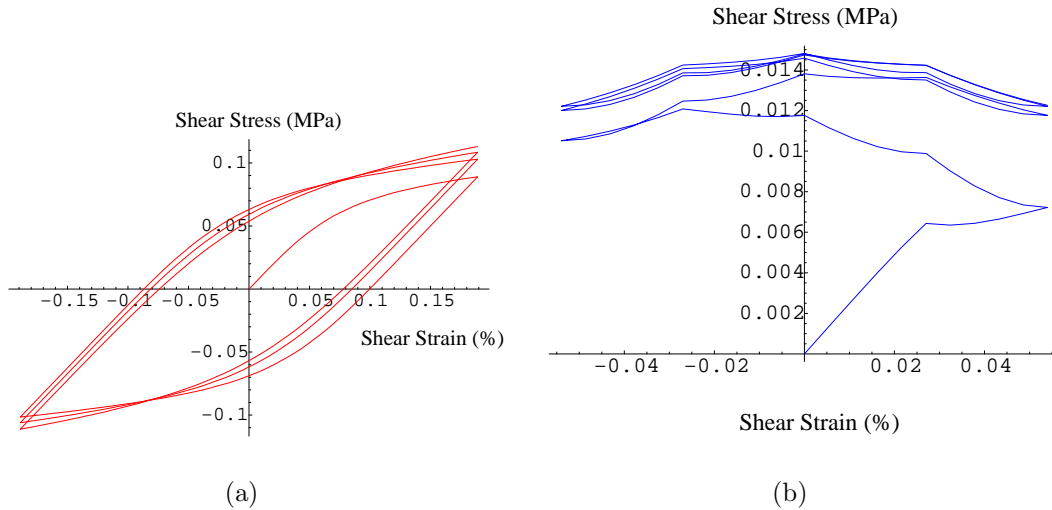


Figure 15. Kinematic hardening probabilistic model under cyclic loading with equal loops: evolution of (a) mean and (b) standard deviation of shear stress

Monotonic loading cases, however, for all probabilistic material models ((i) elastic–perfectly plastic, (Fig. 5), (ii) isotropic linear hardening (Fig. 11), and (iii) linear kinematic hardening (Fig. 16)), are qualitatively similar, with expected differences in rate of hardening.

6. DISCUSSIONS AND CONCLUDING REMARKS

In this paper, a probabilistic framework for macroscopic simulation of geomaterials' behavior is presented, including novel probabilistic yielding concept. It has been shown that, if uncertainties in material parameters are taken into account, a realistic cyclic material behavior could be obtained even with the simple elastic–perfectly plastic probabilistic model. It is also

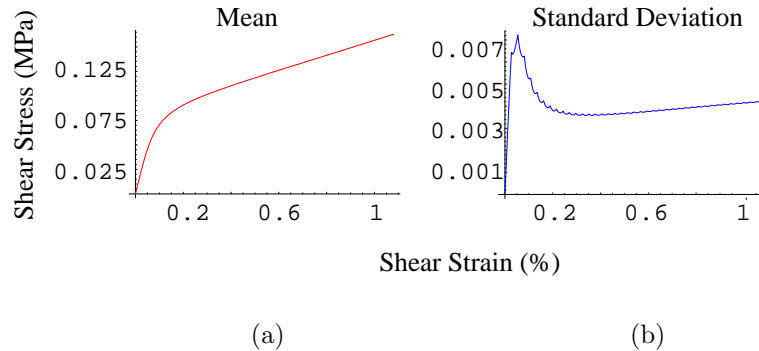


Figure 16. Kinematic hardening probabilistic model under monotonic loading: evolution of (a) mean, (b) standard deviation, and (c) mean \pm standard deviation of shear stress

shown that isotropic or kinematic hardening rule did not significantly improve (if at all) the qualitative nature of the simulated cyclic geomaterial response. These findings seem to nicely support the probabilistic micromechanical simulation results by Einav and Collins [5].

In authors' opinion, probabilistic approach to geomaterial modeling could be very significant in geotechnical engineering. Other than providing a mathematical tool to quantify our confidence in our simulation of geomaterials' behavior, presented approach promises an alternate avenue to geomaterial modeling. By expanding material modeling into probability space, one could simulate realistic geomaterial behavior using simple constitutive models, (elastic–perfectly plastic for example) requiring very few soil parameters that could be easily obtained from in–situ tests, very common in geotechnical practice.

ACKNOWLEDGMENT

The work presented in this paper was supported by a grant from Civil, Mechanical and Manufacturing Innovation program, Directorate of Engineering of the National Science

Int. J. Numer. Anal. Meth. Geomech. 2009; in peer–review:1–31

Foundation, under Award NSF–CMMI–0600766 (cognizant program director Dr. Richard Fragaszy).

REFERENCES

1. Maciej Anders and Muneo Hori. Stochastic finite element method for elasto-plastic body. *International Journal for Numerical Methods in Engineering*, 46:1897–1916, 1999.
2. Maciej Anders and Muneo Hori. Three-dimensional stochastic finite element method for elasto-plastic bodies. *International Journal for Numerical Methods in Engineering*, 51:449–478, 2000.
3. Fischer Black and Myron Scholes. The pricing of options and corporate liabilities. *Journal of Political Economy*, 81(3):637–654, 1973.
4. J. M. Duncan. Factors of safety and reliability in geotechnical engineering. *ASCE Journal of Geotechnical and Geoenvironmental Engineering*, 126(4):307–316, April 2000.
5. Itai Einav and Ian F. Collins. A thermomechanical framework of plasticity based on probabilistic micromechanics. *Journal of Mechanics of Materials and Structures*, 3(5):867–892, May 2008.
6. Federal Highway Administration, U.S. Department of Transportation. Geotechnical engineering circular no. 5. Publication No. FHWA-IF-02-034, April 2002.
7. Gordon A. Fenton and D. V. Griffiths. Probabilistic foundation settlement on spatially random soil. *Journal of Geotechnical and Geoenvironmental Engineering*, 128(5):381–390, May 2002.
8. Gordon A. Fenton and D. V. Griffiths. Bearing capacity prediction of spatially random $c-\phi$ soil. *Canadian Geotechnical Journal*, 40:54–65, 2003.
9. Gordon A. Fenton and D. V. Griffiths. Three-dimensional probabilistic foundation settlement. *Journal of Geotechnical and Geoenvironmental Engineering*, 131(2):232–239, February 2005.
10. Roger G. Ghanem and Pol D. Spanos. *Stochastic Finite Elements: A Spectral Approach*. Dover Publications, Inc., Mineola, New York, 2003.
11. A. C. Hindmarsh, P. N. Brown, K. E. Grant, S. L. Lee, R. Serban, D. E. Shumaker, and C. S. Woodward. SUNDIALS: SUite of Nonlinear and Differential/ALgebraic equation Solvers. *ACM Transactions on Mathematical Software*, 31(3):363–396, 2005.
12. Boris Jeremić and Kallol Sett. On probabilistic yielding of materials. *Communications in Numerical Methods in Engineering*, 25(3):291–300, 2009.

Int. J. Numer. Anal. Meth. Geomech. 2009; **in peer–review**:1–31

13. Boris Jeremić, Kallol Sett, and M. Levent Kavvas. Probabilistic elasto-plasticity: Formulation in 1-D. *Acta Geotechnica*, 2(3):197–210, September 2007.
14. Kari Karhunen. Über lineare methoden in der wahrscheinlichkeitsrechnung. *Ann. Acad. Sci. Fennicae. Ser. A. I. Math.-Phys.*, (37):1–79, 1947.
15. M. Levent Kavvas. Nonlinear hydrologic processes: Conservation equations for determining their means and probability distributions. *Journal of Hydrologic Engineering*, 8(2):44–53, March 2003.
16. Andreas Keese. A review of recent developments in the numerical solution of stochastic partial differential equations (stochastic finite elements). Scientific Computing 2003-06, Department of Mathematics and Computer Science, Technical University of Braunschweig, Brunswick, Germany, 2003.
17. Suzanne Lacasse and Farrokh Nadim. Uncertainties in characterizing soil properties. In Charles D. Shackelford and Priscilla P. Nelson, editors, *Uncertainty in Geologic Environment: From Theory to Practice, Proceedings of Uncertainty 1996, July 31-August 3, 1996, Madison, Wisconsin*, volume 1 of *Geotechnical Special Publication No. 58*, pages 49–75. ASCE, New York, 1996.
18. M. Loève. Fonctions aleatoires du second ordre. Supplement to P. Levy, *Processus Stochastic et Mouvement Brownien*, Gauthier-Villars, Paris, 1948.
19. Hermann G. Matthies, Christoph E. Brenner, Christian G. Bucher, and C. Guedes Soares. Uncertainties in probabilistic numerical analysis of structures and soils - stochastic finite elements. *Structural Safety*, 19(3):283–336, 1997.
20. Kok-Kwang Phoon and Fred H. Kulhawy. Characterization of geotechnical variability. *Canadian Geotechnical Journal*, 36:612–624, 1999.
21. Kallol Sett. Probabilistic elasto-plasticity and its application in finite element simulations of stochastic elastic-plastic boundary value problems. Doctoral Dissertation, University of California, Davis, CA, September 2007.
22. Kallol Sett, Boris Jeremić, and M. Levent Kavvas. Probabilistic elasto-plasticity: Solution and verification in 1-D. *Acta Geotechnica*, 2(3):211–220, September 2007.
23. Kallol Sett, Boris Jeremić, and M. Levent Kavvas. The role of nonlinear hardening/softening in probabilistic elasto-plasticity. *International Journal for Numerical and Analytical Methods in Geomechanics*, 31(7):953–975, June 2007.
24. Kallol Sett, Berna Unutmaz, Kemal Önder Çetin, Suzana Koprivica, and Boris Jeremić. Soil uncertainty and its influence on simulated G/G_{max} and damping behaviors. *Journal of Geotechnical and Geoenvironmental Engineering*, 2008. In review.

25. Mladen Vucetic and Ricardo Dobry. Degradation of marine clays under cyclic loading. *Journal of Geotechnical Engineering*, 114(2):133–149, February 1988.
26. Mladen Vucetic and Ricardo Dobry. Effect of soil plasticity on cyclic response. *Journal of Geotechnical Engineering*, 117(1):133–149, January 1991.
27. N. Wiener. The homogeneous chaos. *American Journal of Mathematics*, 60:897–936, 1938.